

AT CONSTANT SURFACE TEMPERATURE HEAT TRANSFER PERFORMANCE OF SINGLE BLOCKAGES

[Eyüphan MANAY, Veysel ÖZCEYHAN, Bayram ŞAHİN, Kadir GELİŞ]

Abstract— In this study, the effects of equilateral triangular bodies replaced into the channel on heat transfer and flow characteristics were examined numerically. In this research conducted numerically with RNG $k-\epsilon$ method, Reynolds number varied from 5.000 to 10.000. Water was used as working fluid and the constant surface temperature (360K) boundary condition was applied to the bottom wall of the channel. The effects of side length of triangular bodies and Reynolds number were investigated. At the end of the analyses, local and mean Nusselt number, local and mean surface friction factor changes and heat transfer enhancement ratios were given.

Keywords—Bluff body, constant surface temperature, heat transfer enhancement

INTRODUCTION

Bluff bodies are used as a method for enhancing heat transfer and, in related studies the variations, which occur on heat transfer and flow characteristics by the use of the bluff bodies, are investigated. In general, the methods of enhancing heat transfer are divided into two parts as passive and active techniques. In the basic mean, on increasing heat transfer by passive methods, no extra energy is supplied from any outer source, but geometrical parameters of available system is modified in order to increase heat transfer. In active methods, the aim is to enhance heat transfer by supplying extra energy like surface vibrations, suction, pressing. Due to the vibration and acoustic noise problems as well as increasing investment and running costs, energy consumption, increasing heat transfer by active methods have not got attention so much, instead, studies with passive techniques used on cooling of electronics, solar collectors with air, heat recovery units and buildings have intensified.

Eyüphan Manay, Bayram Şahin
Erzurum Technical University, Mechanical Engineering Dep.
Erzurum/ Turkey

Veysel Özceyhan
Erciyes University, Mechanical Engineering Dep.
Kayseri/Turkey

Kadir Geliş
Ağrı İbrahim Çeçen University, Mechanical and Metal Tech.
Ağrı/Turkey

The goal of heat transfer augmentation with passive techniques is to remove viscous sublayer or to destroy in turbulent flow. Because, the elements inserted into the flow field disturb the viscous sublayer and thus, causes it to be destroyed and relative turbulence to occur. This situation increases heat transfer rate among the surfaces with different temperature due to fact that more fluid molecule brushes the surface.

Blockages placed into the flow field or alias bluff bodies not only change the flow structure but also increase heat transfer. Rosales et al. [1] investigated heat transfer and flow characteristics around square cylinders with different dimensions placed into the channel. Once the cylinders were near the channel wall, they concluded that Nusselt number increased, drag force decreased and the highest value of Strouhal number was obtained when the bodies were in the center. Abbassi et al. [2] proposed a model giving the change of Strouhal number with Reynolds number for periodic flow by investigating heat transfer and flow characteristics caused by a triangular element heated externally. Transition from symmetrical form to periodic form was observed at the value of Reynolds number about 45. Furthermore, it was stated that the presence of triangular element in the channel had too low effect on heat transfer and flow shapes for $Re < 45$, there had been remarkable increase in heat transfer at $Re > 45$ (periodic flow) and about 85% increase in heat transfer was provided. Sripattanapipat and Promvong [3] placed diamond shaped elements into the channel. They investigated heat transfer caused as a result of keeping up and down walls at 330K by changing the angles of diamond shaped elements and Reynolds number. Although the use of diamond shaped elements increased heat transfer about 200-680%, 20-220 times higher friction losses than that of smooth channel occurred. Furthermore, it was concluded as a result of the comparison with flat plate that diamond shaped elements increased 6% more heat transfer than flat plate.

Igarashi and Mayumi [4] investigated heat transfer and flow phenomena around rectangle body placed as straight and inclined at Reynolds number range of 2.500-12.800 experimentally. By changing the angle, they defined that the flow was laminar in the case of $\alpha < 15^\circ$ and turbulent in the case of $\alpha \geq 15^\circ$. Furthermore, it was concluded that maximum heat transfer was provided when the angle is in the range of 0° - 5° . Juncu [5], at low Reynolds numbers (1-30), investigated the effects of model parameters on heat transfer for different Prandtl numbers (0.1, 1, 10 and 100) at channel flow around two cylinders placed as tandem. At high values of dimensionless temperatures of the cylinders, high heat transfer rates were achieved once the interaction started and

developed. They stated that this was obtained as a result of high convection rate, small gap ratios between the cylinders and high values of volumetric heat capacity. Mahir and Altaç [6] investigated convective heat transfer at tandem arrangement and transient flow regime for different gap ratios ($L/D=2, 3, 4, 5, 7$ and 10). In the numerical study conducted at two different Reynolds numbers, the flow characteristics were also presented. In the case of $L/D \geq 4$, Nusselt number of the front cylinder rised to that of a single one. For $L/D \geq 4$, heat transfer rate in rear cylinder became 80% of front cylinder while this phenomena occured at the front cylinder.

Meinders and Hanjalic [7] investigated heat transfer between two cubes placed as tandem and staggered onto the bottom in fully developed flow field. Likewise, flow characteristics were also investigated. While flow patterns and heat transfer were periodic in case of tandem arrangement, they showed different asymmetrical flow patterns. Nakamure et al. [8] researched flow and heat transfer parameters around cube placed with 45° into the flow field for different cube heights and Reynolds numbers. At the end of the analyses, it was stated that heat transfer distribution were highly different at arrangement with angle than that of straight one, high heat transfer and low pressure regions were formed by reattachment and separation lines. The heat transfer and flow characteristics around heated square cylinder were studied by Turki et al. [9]. Together with the heating of square cylinder placed into the channel, they investigated the variations occurring on heat transfer and flow field by the change of blockage ratio ($\beta=1/4$ and $1/8$), Reynolds and Richardson numbers. I was observed that the critical value of the Reynolds number increased by the increase of blockage ratio on transition from steady flow to periodic flow, the total heat transfer from square cylinder is slightly affected from blockage ratio. It was defined that the critical value of Reynolds number on transition from steady to periodic flow decreased with increasing Richardson number.

In this present study, differently from literature flow and heat transfer characteristics belonging to the flow field of triangular bodies were investigated numerically by inserting triangular elements with different lengths into the flow field.

CFD ANALYSIS

A. Problem Description

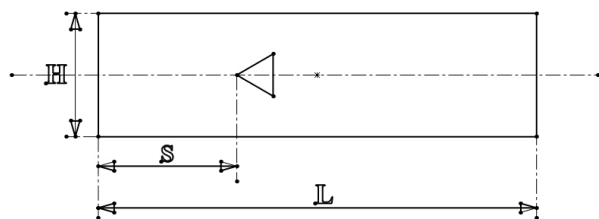


Figure 1. Computational domain and the triangular bodies.

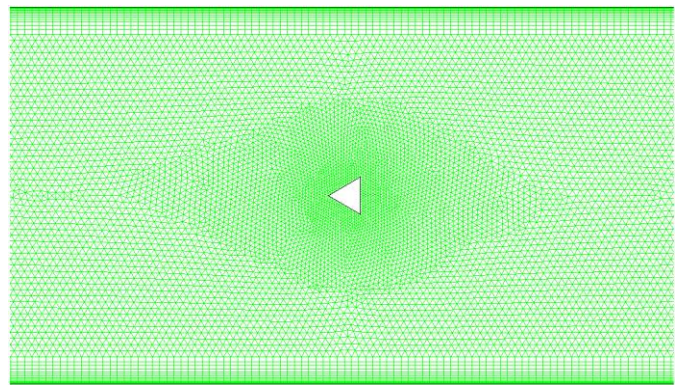


Figure 2. Mesh structure of equilateral triangular blockage.

In Figure 1, the main features of the test section are shown schematically. The computational domain mainly consists of two-dimensional channel and triangular bodies. As seen in Figure 1, channel height (H) of $4B$, the placement of the bluff bodies (S) was maintained at $x = 8B$, while the channel length was $36B$. For preventing from the negative pressure effects at the outlet sections the outlet section was selected long enough, likewise the inlet section was selected long enough to get a fully developed flow.

In the present study, on the brink of showing the mesh independency four different mesh numbers were tried, for comparison, radial velocity variations in x direction were given in Figure 3. Mesh structure was also shown in Figure 2. According to the velocity variations determined at $x/L=0.5$, the mesh structure of 1070×66 could not be enough for solution. The velocity variation on mesh structure of 1426×78 used in this study showed similarity with that of 2140×101 . Because no change was observed after this mesh number, the mesh number of 1426×78 was used in this study.

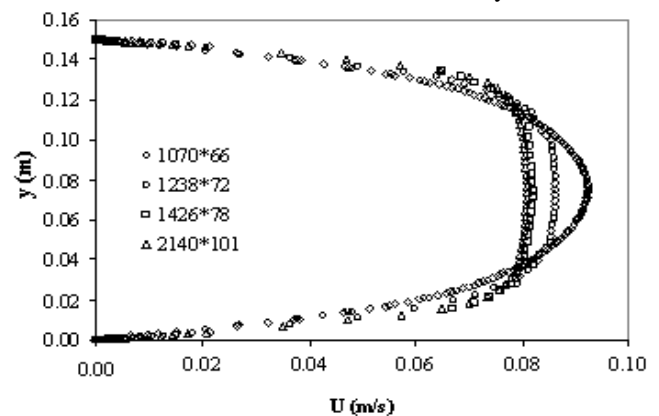


Figure 3. Velocity variations at different mesh numbers.

Numerical Procedure

For determining the temperature distributions, CFD calculations made by the aid of the computational fluid dynamics (CFD) commercial code of FLUENT version 6.1.22 [11] are performed depending on the numerical model, boundary conditions, assumptions, and numerical values. In all

the numerical calculations, segregated manner was selected as solver type, due to its advantage which helps to prevent from convergence problems and oscillations in pressure and velocity fields of strong coupling between the velocity and pressure by using. (RNG) k-ε turbulence model is used for simulations and the second order upwind numerical scheme and SIMPLE algorithm being more stable and economical in comparison with the other algorithms are utilized to discretize the governing equations. The converging criterions are thought as 10⁻⁶ for the energy and 10⁻⁴ for other parameters. In momentum and continuity equations, the thermophysical properties are thought as constant, and, the flow is assumed two-dimensional, steady state.

Continuity conservation:

$$\frac{\partial \rho}{\partial t} + \nabla \cdot (\rho \cdot \vec{v}) = 0 \quad (1)$$

Momentum conservation:

$$\frac{\partial (\rho \cdot \vec{v})}{\partial t} + \nabla \cdot (\rho \cdot \vec{v} \cdot \vec{v}) = \rho \vec{g} - \nabla P + \nabla \cdot (\vec{\tau}) \quad (2)$$

Energy conservation:

$$\frac{\partial (\rho E)}{\partial t} + \nabla \cdot (\vec{v} \cdot (\rho E + p)) = \nabla \cdot (k_{eff} \nabla T + (\vec{\tau}_{eff} \cdot \vec{v})) \quad (3)$$

In Eqs. 2, 3 and 4, v is the velocity, P is the pressure, T is the temperature, ρ is the density of air. u , v and w are the velocity components in the direction of x , y and z in Cartesian coordinate system, respectively. The above thermo-physical properties of water are taken as temperature independent (constant) properties. Because of the fact that the flow is fully turbulent, the turbulent kinetic energy and the dissipation rate of turbulent kinetic energy equations derived from the transport equations are given as below:

$$\frac{\partial}{\partial t}(\rho k) + \frac{\partial}{\partial x_i}(\rho k u_i) = \frac{\partial}{\partial x_j} \left(\alpha_k \mu_{eff} \frac{\partial k}{\partial x_j} \right) + \quad (4)$$

$$G_k + G_b - \rho \varepsilon - Y_M + S_k$$

$$\frac{\partial}{\partial t}(\rho \varepsilon) + \frac{\partial}{\partial x_i}(\rho \varepsilon u_i) = \frac{\partial}{\partial x_j} \left(\alpha_\varepsilon \mu_{eff} \frac{\partial \varepsilon}{\partial x_j} \right) + C_{1\varepsilon} \frac{\varepsilon}{k} (G_k + C_{3\varepsilon} G_b) \quad (5)$$

$$- C_{2\varepsilon} \rho \frac{\varepsilon^2}{k} - R_\varepsilon + S_\varepsilon$$

In these equations, G_k represents the generation of turbulence kinetic energy due to the mean velocity gradients, G_b is the generation of turbulence kinetic energy due to buoyancy. Y_M represents the contribution of the fluctuating dilatation in compressible turbulence to the overall dissipation rate. The quantities α_k and α_ε are the inverse effective Prandtl numbers for k and ε , respectively. S_k and S_ε are user-defined source terms. In RNG k-ε turbulence model, the turbulent viscosity is calculated by Eq. 6,

$$d \left(\frac{\rho^2 k}{\sqrt{\varepsilon} \mu} \right) = 1.72 \frac{\hat{v}}{\sqrt{\hat{v}^3 - 1 + C_v}} d \hat{v} \quad (6)$$

where, $C_v \approx 100$

$$\hat{v} = \mu_{eff} / \mu \quad (7)$$

In high Reynolds numbers, the effective viscosity is calculated via Eq. 9

$$\mu_t = \rho C_\mu \frac{k^2}{\varepsilon} \quad (8)$$

with $C_\mu = 0.0845$, derived using RNG theory. It is interesting to note that this value of C_μ is very close to the empirically-determined value of 0.09 used in the standard k-ε model [11]. The Eq. 9 presented below is used for the calculation of the inverse effective Prandtl numbers, α_k ve α_ε ,

$$\left| \frac{\alpha - 1.3929}{\alpha_0 - 1.3929} \right|^{0.6321} \left| \frac{\alpha + 2.3929}{\alpha_0 + 2.3929} \right|^{0.3679} = \frac{\mu_{mol}}{\mu_{eff}} \quad (9)$$

where, $\alpha_k = 1.0$. In high Reynolds numbers ($\mu_{mol} / \mu_{eff} \ll 1$), $\alpha_k = \alpha_\varepsilon \approx 1.393$ [11]. The main difference between the RNG and standard k-ε models lies in the additional term in the ε equation given by FLUENT 6.1.22.

B. Model Constants

$C1\varepsilon$, $C2\varepsilon$ model constants are obtained analytically by the RNG theory, $C1\varepsilon=1.42$, $C2\varepsilon=1.68$, (FLUENT 6.1.22). Two parameters of interest for this study are the skin friction coefficient and the Nusselt number. The skin friction coefficient C_f is defined by

$$C_f = \frac{\tau_s}{\frac{1}{2} \rho U_m^2} \quad (10)$$

The heat transfer performance is evaluated by Nusselt number which can be obtained by the local temperature gradient as:

$$Nu = - \frac{\partial T}{\partial Z} \quad (11)$$

The average Nusselt number can be calculated as follows:

$$Nu_{av} = \int Nu_x \frac{\partial x}{L} \quad (12)$$

where L is the length of computational domain. The friction factor is determined from; in which pressure ΔP is pressure difference between the channel inlet and exit.

$$f = \frac{\Delta P}{\frac{1}{2} \rho U_m^2 \frac{L}{H}} \quad (13)$$

Boundary Conditions

The solution domain of the considered 2D channel flow is geometrically quite simple, which is a rectangle on the $x-z$ plane, enclosed by the inlet, outlet and wall boundaries. The working fluid in all cases is water. The inlet temperature of water is considered to be uniform at 300 K. On walls, no-slip conditions are used for the momentum equations. A constant surface temperature of 360 K is applied to the bottom wall of the channel. The upper wall is assumed to be adiabatic. Uniform velocity is imposed to inlet plane and the Reynolds number varies from 5.000 to 10.000. The outlet boundary condition is natural condition which implies zero-gradient conditions at the outlet.

RESULTS

For the purpose of using in heat transfer characteristics analyses Nusselt number variations belonging to bottom wall, surface friction factor coefficient variations along the bottom wall, average Nusselt number and surface friction factors with Reynolds number have been presented. Nusselt number variations along the bottom wall are shown in Figure 4a, b and c. Because Nusselt number directly represents heat transfer, length of the edges of triangular bodies and Reynolds number are important parameters with respect to Nusselt number.

In all arrangements, Nusselt number increases once the fluid faces with the triangular obstacles and passes them. As understood from the graphs at the first meeting point with the obstacles, Nusselt number takes a peak value. But, Nusselt number does not decrease directly due to the disturbing the flow and thus boundary layer, decreases by fluctuating. As seen in Figure 4, in case of $B=15$ mm Nusselt number does not increase so much due to the fact that the flow could not be disturbed sufficiently, but at $B=25$ mm increases much more than that of $B=15$ and $B=20$ mm because of the mentioned reason. In the basic mean, the investigation of heat transfer enhancement by placing triangular bodies into the channel without giving no extra energy from outside is the process of heat transfer enhancement via passive methods. Upon increasing heat transfer via passive methods, an undesired situation is that the friction increases, in other words pump load increases.

In Figure 5a, b and c, the variations on surface friction coefficient along the bottom wall are presented in the case of adding inner elements into the channel flow. Fundamentally, what causes heat transfer and friction to increase is the behaviour of the fluid in molecular level. Because they are based on the same basis, the variation trend of surface friction coefficient along the bottom wall is similar to that of Nusselt number. Average Nusselt number variations with Reynolds number are shown in Figure 6. From general heat transfer knowledge, it is an expected situation that Nusselt number increases with the increase of Reynolds number. In case of

changing the edge lengths of triangular bodies, the highest Nusselt number is obtained at $B=25$ mm and $Re=10.000$. In figure 7, the variations of surface friction factor along the bottom wall of the channel with Reynolds factor are presented in case of placing equilateral triangular bodies into the channel. In all cases, Surface friction factor decreases with the increase of Reynolds number. The lowest surface friction factor is obtained at $B=15$ mm and $Re=10.000$.

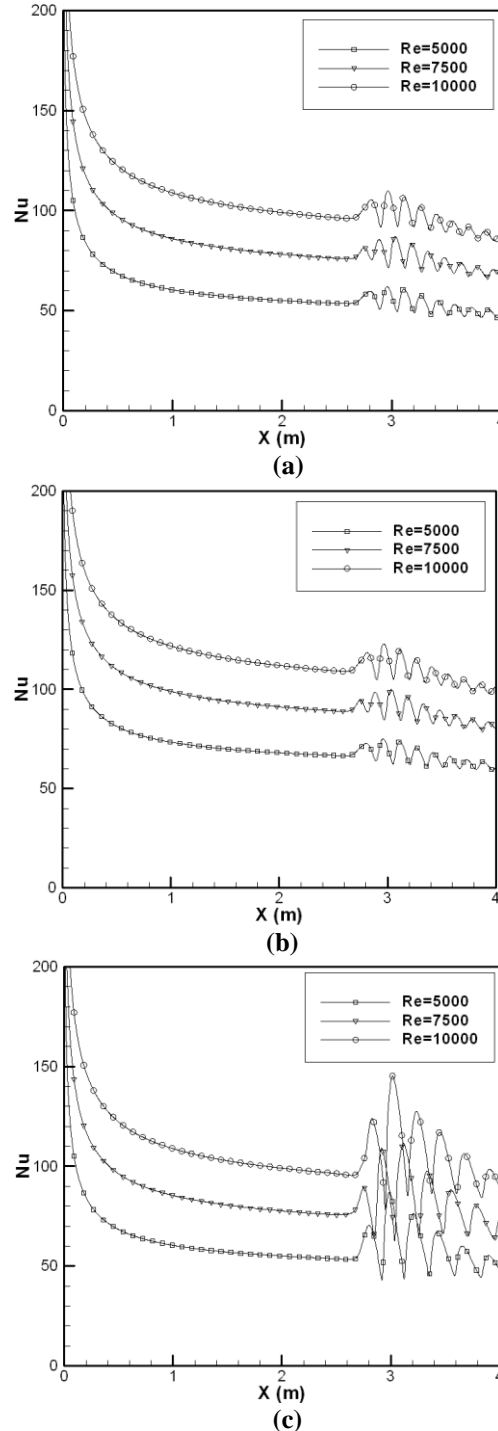


Figure 4. Nusselt number variations for triangular bodies, (a) $B=15$ mm, (b) $B=20$ mm, (c) $B=25$ mm.

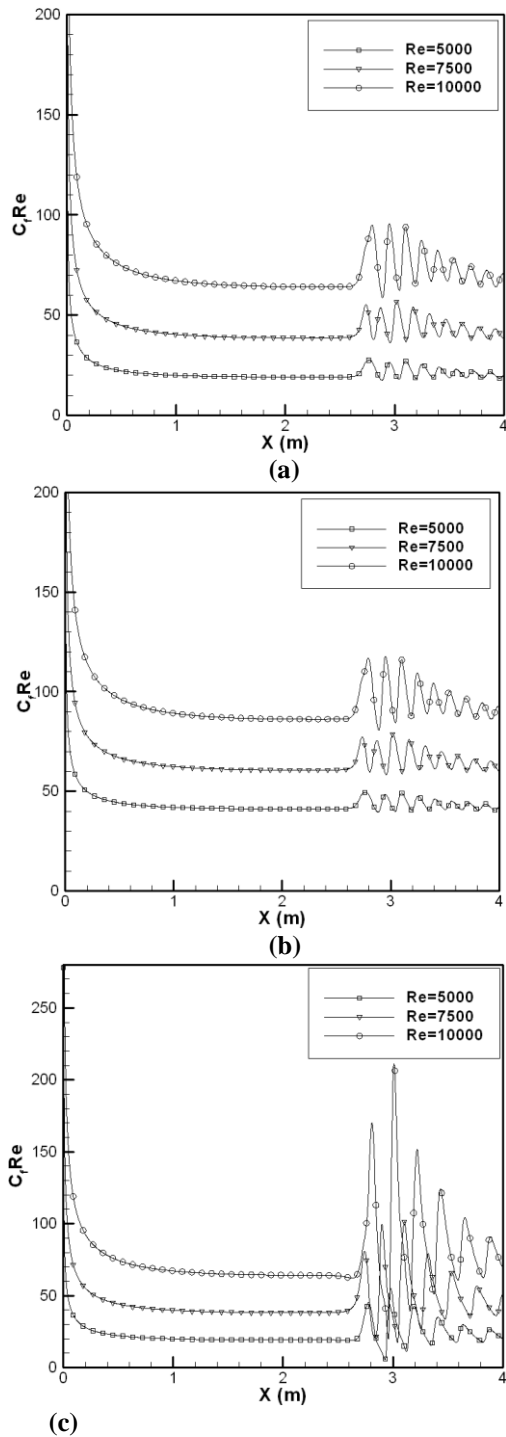


Figure 5. Surface friction factor variations along the bottom wall of the channel, (a) $B=15$ mm, (b) $B=20$ mm, (c) $B=25$ mm.

In the present study, overall heat transfer enhancement is presented for all cases in Figure 8. In the present graphics, for better understanding the overall heat transfer enhancement axis is given in the range of 0.5-1.5. With the help of the calculated results, it is concluded that the overall heat transfer enhancement is provided for the cases higher than 1. In order to know whether overall heat transfer enhancement is provided

or not, Nusselt number and friction factor values must be calculated. For that reason, numerical studies in smooth channel are performed. Among three edge lengths of triangular bodies, the overall heat transfer enhancement is only obtained at $Re=5.000$ for each body while no heat transfer enhancement is obtained at $Re=7.500$ and $Re=10.000$. The highest heat transfer enhancement is achieved in the case of $B=25$ mm and $Re=5.000$. Likewise, the lowest one is achieved in the case of $b=25$ mm and $Re=10.000$.

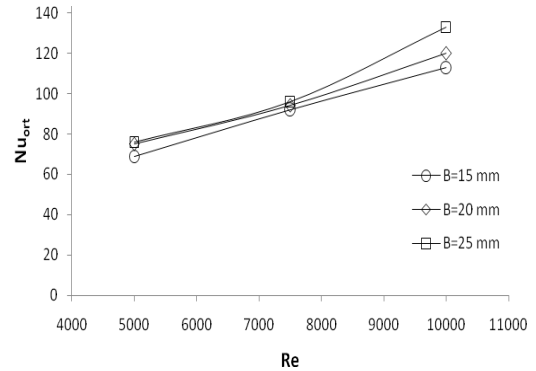


Figure 6. Average Nusselt number variations versus Reynolds number

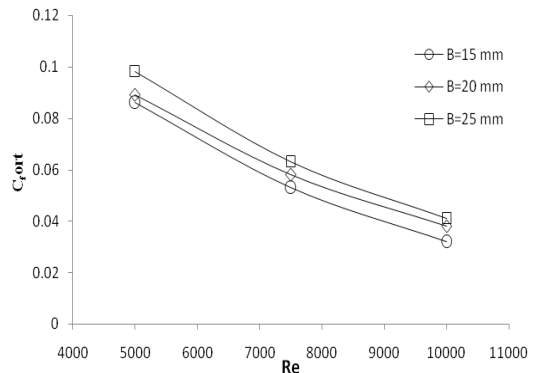


Figure 7. Average surface friction coefficient variations versus Reynolds number.

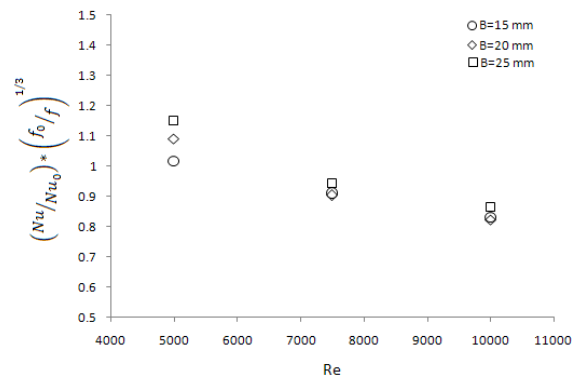


Figure 8. Overall heat transfer enhancement versus Reynolds number.

CONCLUSIONS

In this numerical study, forced convective heat transfer and pressure drop characteristics of equilateral triangular bodies placed into the rectangle channel were analysed. For that reason, Nusselt number variations belonging to the bottom wall, surface friction factor coefficient variations along the bottom wall, average Nusselt number and surface friction factors with Reynolds number were presented. The remarkable conclusions were sequenced. In case of $B=15$ mm Nusselt number did not increase so much due to the fact that the flow could not be disturbed sufficiently, but at $B=25$ mm increased much more than that of $B=15$ and $B=20$ mm. Nusselt number increased with the increase of Reynolds number. The highest Nusselt number was obtained at $B=25$ mm and $Re=10.000$. The lowest surface friction factor was obtained at $B=15$ mm and $Re=10.000$. The overall heat transfer enhancement was only obtained at $Re=5.000$ for each body while no heat transfer enhancement was obtained at $Re=7.500$ and $Re=10.000$. The highest heat transfer enhancement was achieved in the case of $B=25$ mm and $Re=5.000$.

References

- [1] Rosales, J. L., Ortega, A. and Humphrey, J. A. C., A Numerical Simulation of the Convective Heat Transfer in Confined Channel Flow Past Square Cylinders: Comparison of Inline and Offset Tandem Pairs, *International Journal of Heat and Mass Transfer*, 44: 587-603, 2001.
- [2] Abbassi, H., Turki, S. and Nasrallah, S.B., Numerical investigation of Forced Convection in a Plane Channel with a Built-in Triangular Prism, *International Journal of Thermal Sciences*, 40: 649-658, (2001).
- [3] Sripattanapipat, S. and Promvongse, P., Numerical Analysis of Laminar Heat Transfer in a Channel with Diamond-Shaped Baffles, *International Communications in Heat and Mass Transfer*, 36: 32–38, 2009.
- [4] Igarashi, T. and Mayumi, Y., Fluid Flow and Heat Transfer Around a Rectangular Cylinder with Small Inclined Angle., *International Journal of Heat and Fluid Flow*., 22: 279-286, 2001.
- [5] Juncu, G., A Numerical Study of Momentum and Forced Convection Heat Transfer Around Two Tandem Circular Cylinders at Low Reynolds Numbers. Part II: Forced Convection Heat Transfer, *International Journal of Heat and Mass Transfer*, 50: 3799–3808, 2007.
- [6] Mahir, N. and Altaç, Z., Numerical Investigation of Convective Heat Transfer in Unsteady Flow Past Two Cylinders in Tandem Arrangements, *International Journal of Heat and Fluid Flow*, 29: 1309–1318, 2008.
- [7] Meinders, E. R. and Hanjalic, K., Experimental Study of the Convective Heat Transfer form In-line and Staggered Configurations of Two Wall-Mounted Cubes, *International Journal of Heat and Mass Transfer*, 45: 465-482, 2002.
- [8] Nakamura, H., Igarashi, T. and Tsutsui, T., Local Heat Transfer Around a Wall-Mounted Cube at 45o to Flow in a Turbulent Boundary Layer, *International Journal of Heat and Fluid Flow*, 24: 807–815, 2003.
- [9] Turki, S., Abbassi, H. and Nasrallah, S. B., Two-Dimensional Laminar Fluid Flow and Heat Transfer in a Channel with a Built-in Heated Square Cylinder, *International Journal of Thermal Sciences*, 42: 1105–1113, 2003.
- [10] Manay, E., “İçerisine üçgen iç elemanlar yerleştirilmiş kanalda ısı transferi ve akış karakteristiklerinin deneysel ve sayısal olarak incelenmesi”, Yüksek lisans tezi, Erciyes Üniversitesi, 2010.
- [11] FLUENT 6.1.22., “User’s Guide”, Fluent Incorporated, Centerra Resource Park, 10 Cavendish Court, Lebanon, NH 03766, USA, 2001.